Available online at www.sciencedirect.com

SCIENCE DIRECT

Cement and Concrete Research 35 (2005) 2158 – 2164

Cement and Concrete Research

Preliminary evaluation of MEMS devices for early age concrete property monitoring

Mohamed Saafi*, Peter Romine

Center for Transportation Infrastructure Safety and Security Alabama A&M University Normal, AL 35762-0818, USA

Received 20 February 2005; accepted 29 March 2005

Abstract

Early age concrete properties and strength gain are mainly related to the hydration of cement and moisture transfer. In this paper we will present a new technique that is currently under development for monitoring concrete setting and hardening. The new monitoring technique consists of embedding MicroElectroMechanical System (MEMS) devices into concrete during construction to wirelessly monitor certain key parameters affecting the early age behavior of concrete structures such as in-place strength and shrinkage stresses. To test the feasibility of the proposed devices in monitoring temperature, moisture and early age shrinkage stresses as well as to evaluate their durability when embedded into concrete, experimental tests were performed and preliminary results are presented in this paper.

Keywords: Curing; Humidity; Temperature; Shrinkage; MEMS sensors

1. Introduction

Accurate field measurements of early age concrete properties, such as setting time, in-place strength gain and shrinkage stresses are crucial to operation scheduling and in situ quality control of concrete. For example, reliable measurements of in-place concrete strength can be used to determine when adequate strength has been obtained to allow removal of forms, shoring, transfer of prestressing, application of post-tensioning and opening highways to traffic. In-place strength information allows each of these operations to proceed safely and at the earliest possible time leading to more economical construction. The development of concrete strength at early age mainly depends on the moisture diffusion and hydration temperature. Rapid loss of moisture could lead to insufficient strength development which in return could lead to the development of damage in concrete structures prior to loading [1]. At an early age, concrete structures can also be subjected to deformation during the hydration process mainly due to moisture loss and hydration temperature [2]. If in the cooling phase, contraction of the concrete is hindered, tensile stresses are generated in the structure. These tensile stresses cause cracking when exceeding the tensile strength of the hardening concrete. Consequently, in situ measuring of early age shrinkage stresses can be used to estimate when shrinkage stresses begin to be generated as well as to estimate self-stressing and risk of premature cracking [3]. When structures are constructed in successive phases, these measurements can help to improve the composition of concrete when necessary. Thus, it is very important to monitor the temperature and moisture distribution in concrete structures and shrinkage stresses to evaluate the setting and hardening process of Portland cement concrete for early age concrete strength gain monitoring and to evaluate the severity of shrinkage induced cracks.

Current monitoring techniques are mainly based on surface measurements and are expensive, time consuming, and require major equipment and labor intensive to operate them and to gain access to remote locations in the structure. Rapid advancement in microscience over the last decade has led to the development of microtechnology as a new

* Corresponding author. Tel.: +1 256 372 4114; fax: +1 256 372 5586.
E-mail address: mohamed.saafi@email.aamu.edu (M. Saafi).

0008-8846/$ - see front matter © 2005 Elsevier Ltd. All rights reserved.
doi:10.1016/j.cemconres.2005.03.012

enabling technology for new cost-effective, durable, reliable and wireless devices that can be embedded into concrete structures for durability and health monitoring. However, despite the potential benefits of this emerging technology, its application in civil engineering is currently nonexistent due to the lack of research in this area. When embedded into concrete, these devices will increase the understanding of the hydration process and damage evolution of concrete structures. Embedded microsensors could also be used to detect crack initiation in concrete structures under loading or to monitor the setting of concrete by detecting the development of hydration products. The incorporation of microdevices in concrete material would allow for real-time health monitoring of the structure and provide information on durability and early damage detection.

The paper studies the feasibility of embedding MEMS devices into concrete to monitor its early age properties such as temperature, moisture and shrinkage induced stresses. Experimental tests were carried out to evaluate the effect of concrete curing on the MEMS response and the capability of these devices in measuring temperature, moisture content and shrinkage stresses.

2. Preliminary experiments

2.1. MEMS sensors design

Preliminary experiments were carried out to evaluate the feasibility of embedding MEMS devices into concrete for moisture, temperature and shrinkage stress monitoring as well as to evaluate the durability and survivability of these devices in a concrete corrosive environment. The curing and damage process of concrete is significantly affected by the temperature and moisture level. Therefore, a sensor system for continuous monitoring of internal relative humidity and temperature is highly desirable for both during construction and afterwards. The proposed MEMS sensor for internal humidity and temperature consists of four bulk micromachined microcantilever beams (120×380 μm) equipped with a moisture sensitive thin polymer and a microstrain gauge and it is capable of measuring simultaneously temperature and moisture in concrete. The detailed technical description of this MEMS device can be found in [4]. During sensor operation, ambient water vapor molecules adsorb onto the sensing film surface. These molecules are held there by weak van der Waals force due to the polar nature of the water molecule. The water molecules continue to form polar bonds with various radical groups of the polymer molecules with the film and take up space thereby displacing the polymer molecules, resulting in bulk dimensional changes of the sensing film. All of the free surfaces of the film displace parallel and normal to the adjacent microbeam surfaces, with exception of the film surface that is bonded to each cantilever beam. The bond constrains this film surface, preventing it from displacement. This constraint, known as a full shear constraint, produces shear stresses at the film/beam interface which cause the cantilever beam to deflect. This deflection is measured as a resistance change in the embedded strain gauges and is linearly proportional to the shear stress. Consequently, the water vapor concentration is transduced into a proportional differential voltage change in the bridge circuit.

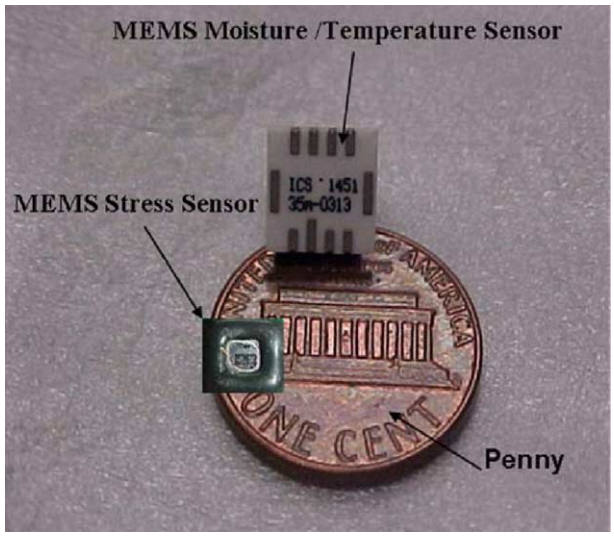

Fig. 1. Packaged MEMS sensors.

To measure concrete shrinkage stress during curing as well as concrete stresses generated by external load when the structure is in service, MEMS stress sensors were also designed. The stress sensor is composed of eight microsensor rosettes patterned on n-type (111) silicon membrane of 2 mm × 2 mm with a total thickness of 8 μm and an on-chip temperature sensor. The detailed technical description of this MEMS device can also be found in [4]. The two principal shrinkage stresses σ_{11} and σ_{22} were calculated using a developed piezoresistive theory [4]. To measure temperature, an on-chip semiconductor (thermistor) temperature sensor is bonded to the top of the chip.

The MEMS sensors were fabricated and packaged for concrete application. As shown in Fig. 1, the moisture/temperature sensors were encapsulated with stainless jackets equipped with a ceramic filter for sensing purposes and the stress sensors were encapsulated with a high strength thin film polymer. The sensors outputs were monitored continuously using a data acquisition system with wire connections for proof of concept.

3. Experimental program

3.1. MEMS temperature/moisture sensor calibration

The MEMS temperature/moisture responses were evaluated to study the repeatability, hysterisis property and temperature dependency. In total, 10 MEMS sensors were evaluated using a controlled humidity chamber and sub-

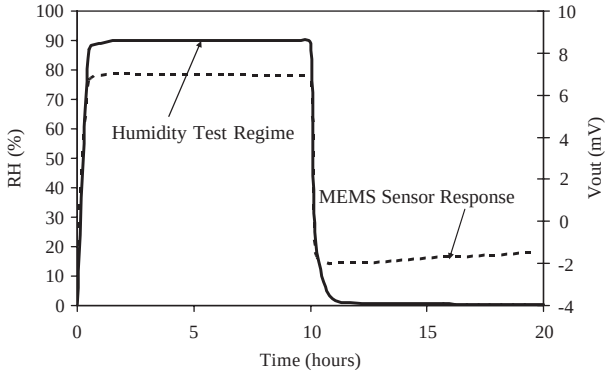

Fig. 2. Humidity test regime and MEMS moisture response at temperature=25 °C.

jected to an excitation of 2 V. As shown in Figs 2 and 3, each MEMS was subjected to a relative humidity (RH) regime at a constant temperature of 25 °C and 65 °C. The RH was increased from 0.5% to approximately 90% and kept constant for a period of 10 h then decreased to 0.5% RH and remained constant for a period of 10 h. In addition, the MEMS devices were subjected to a cyclic RH regime at a constant temperature of 35 °C to evaluate their recovery time and repeatability as shown in Fig. 4. The MEMS devices were also subjected to RH cycles to determine their hysteresis. The hysteresis of these devices was defined as the maximum difference between two RH cycles, 6–90% and 90–6%. Cycling was performed in 20% RH increments with a stabilization time of 5 min after each increment and at a predetermined temperature.

Figs. 2 and 3 show typical MEMS outputs in response to RH regimes. It was found that MEMS devices exhibited response similar to the RH regime with excellent repeatability. However, there was a slight change in the sensors response after 4 h of exposure due to high temperature (specimens subjected to 65 °C), indicating that the effect of temperature should be incorporated in the sensor response. The effect of RH regime cycles on the MEMS response is depicted in Fig. 4. As can be seen from this figure, the MEMS exhibited rapid recovery time and good repeatability. Fig. 5 shows a typical MEMS hysteresis curve after

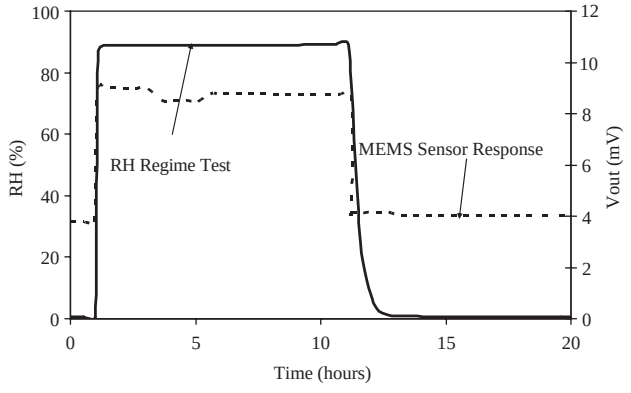

Fig. 3. Humidity test regime and MEMS moisture response at temperature=65 °C.

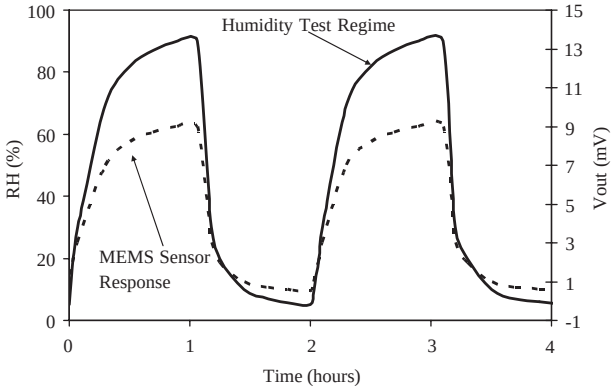

Fig. 4. Cyclic humidity test regime and MEMS moisture response.

RH cycles where a good linearity between the sensors output and RH is obtained. The average hysteresis of tested devices was between 1% and 3% FS (full scale). During these tests, the MEMS temperature sensors were also calibrated and Table 1 summarizes the MEMS characteristics and calibration data. The obtained preliminary calibration equations for temperature and humidity measuring are:

$$\%\ \mathrm{RH} = \frac{0.5V_{\mathrm{RH}} + 0.03}{1.0546 - 0.00216T} \times 100 \tag{1}$$

$$T(\mathrm{deg\ C}) = 64.39V_{\mathrm{T}} + 20.23 \tag{2}$$

where V_{RH} and V_{T} are the MEMS outputs in volts for humidity and temperature, respectively, and T is the measured concrete temperature.

3.2. Preliminary tests on MEMS embedded into concrete specimens

Concrete cylinders of 152 mm × 305 mm with water to cement ratio of 0.45 and 0.53 were used to evaluate the performance of the MEMS moisture/temperature sensor. Each MEMS was embedded in the middle of the specimen and placed in a curing room at room temperature of approximately 21 °C at RH=50. In addition, concrete beams of 100 mm × 100 mm × 450 mm with a water to

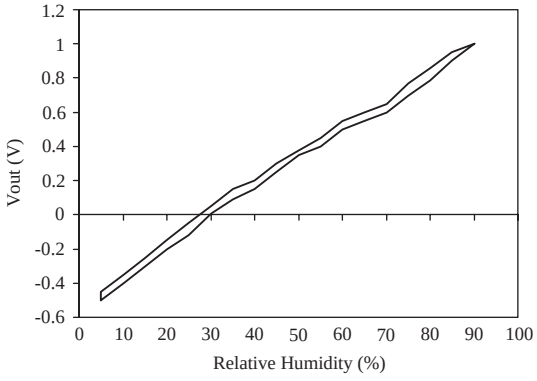

Fig. 5. Typical MEMS moisture hysteresis curve.

Table 1
MEMS temperature/moisture sensor characteristics

Parameter	Specification	Units
Excitation voltage	1.2	V
Current	0.7	mA
Moisture Sensor		
Gain	0.5	%RH/mV
Offset	0.03	%RH
Linearity	0.997	R^2
Hysteresis	1 (min), 3 (max)	%FS
Time Response	< 8	s
Temperature Sensor		
Gain	64.39	°C/V
Offset	20.23	°C
Linearity	0.998	R^2

cement ratio of 0.5 were used to evaluate the capability of the MEMS stress sensor in measuring shrinkage stresses. Each stress sensor was embedded in the middle of each beam to measure longitudinal and transversal shrinkage stresses. Fig. 6 shows the location of the embedded stress sensors and orientation of the resistors with respect to the longitudinal and transversal axes of the beams. The concrete beams were removed from molds after 5 h of curing to accelerate the shrinkage. The moisture, temperature and shrinkage stresses were monitored continuously using a data acquisition system with wire connections for proof of concept.

4. Preliminary results

4.1. MEMS response when embedded into concrete specimens

Figs. 7 and 8 show typical voltage outputs of the MEMS moisture/temperature sensor for the first 20 days of curing when embedded into the concrete cylinders. Concrete temperature and room temperature recorded by thermocouples are also shown in the figures. As can be seen in Fig. 7, the temperature output voltage increased to its maximum of 0.15 V after 10 h of curing. This maximum voltage corresponds to the peak of the maximum temperature generated by the hydrated cement paste. The output voltage then decreased and remained constant with voltage peaks due to the change in the room temperature as evidenced by the thermocouple outputs. Fig. 7 revealed that the sensor output and concrete temperature recorded by the thermocouple exhibited a similar trend. Fig. 8 shows the response of the MEMS humidity sensor where the demolding initiated a brief drop in the sensor output at a time of 1 day. After the temperature and vapor pressure reached equilibrium, the output voltage increased reaching its maximum after 2 days before gradually decreasing as drying occurred. Fig. 8 also shows that the internal concrete temperature affected the sensor output where the sudden drop in the internal concrete temperature generated sensor output voltage peaks. The MEMS temperature and humidity responses are shown in Figs. 9 and 10 for a water to cement ratio of 0.45 and 0.53. As expected, specimens with water to cement ratio of 0.53 exhibited a higher voltage response

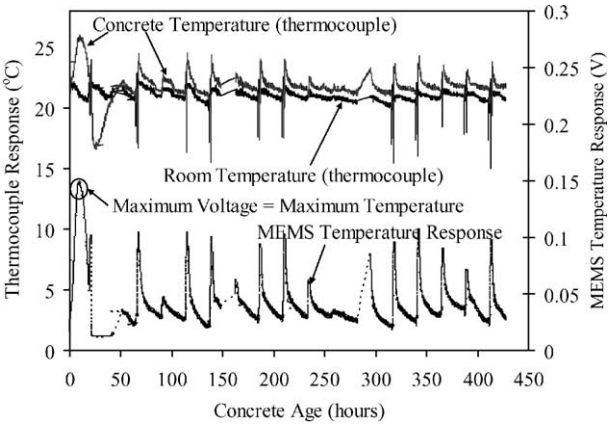

Fig. 7. Typical embedded MEMS temperature response.

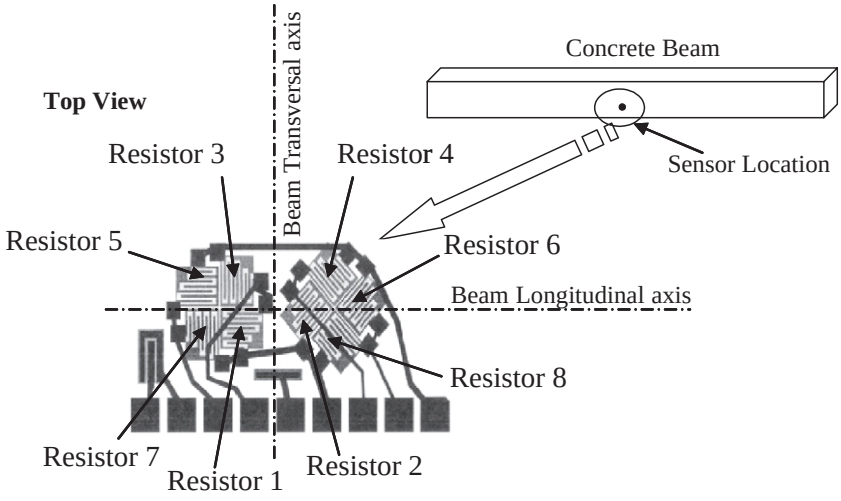

Fig. 6. MEMS stress sensor location (top view).

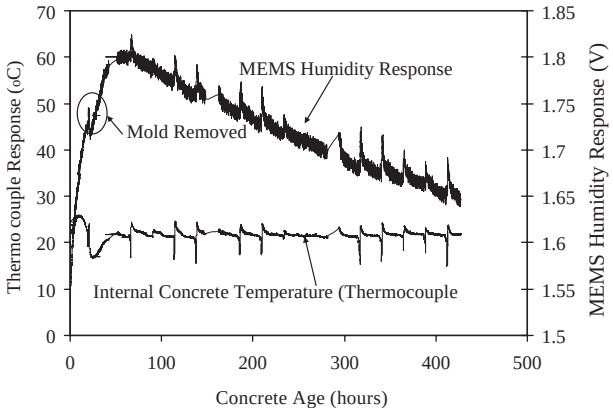

Fig. 8. Typical embedded MEMS moisture response.

during the hydration process than those with a water to cement ratio of 0.45. However, water to cement ratio appeared to have no significant influence on the temperature sensor response after the main hydration process is completed. Water to cement ratio has no effect on the MEMS humidity response during the first 48 h, however sensor outputs from concrete cylinders with a water to cement ratio of 0.53 were slightly higher than those from concrete cylinders with a water to cement ratio of 0.45 after 48 h of curing. This response is mainly due to the fact that the amount of water in specimens with relatively low water to cement ratios (0.45) is slightly lower than that in specimens with water to cement ratio of 0.53. The glitches present in the MEMS humidity responses (Fig. 10) were due to unrecorded data caused by the malfunction of the data acquisition system.

The response of the embedded MEMS stress sensor due to free shrinkage is given by Fig. 11. In this figure, the change in the resistance of the resistors and concrete temperature are presented. As can be seen, there was a positive increase in the resistance of each resistor up to a maximum value, then remained constant for a period of 10 hours before gradually decreasing (negative increase) as drying occurred. The increase in the resistances is attributed

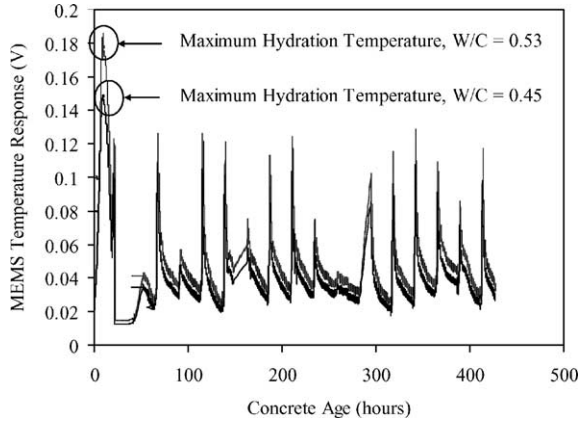

Fig. 9. Typical MEMS temperature sensor response for different water/cement ratios.

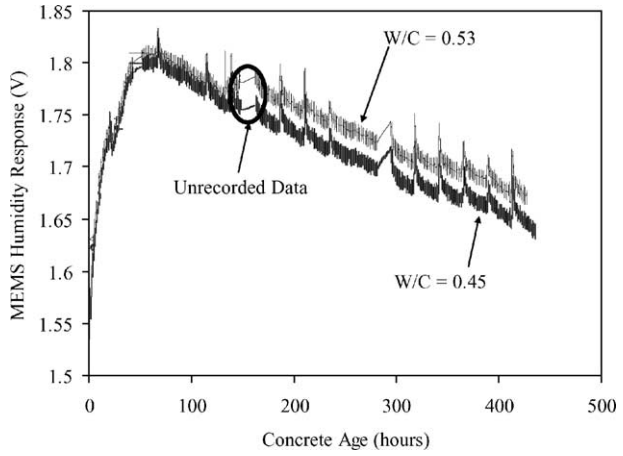

Fig. 10. Typical MEMS moisture sensor response for different water/cement ratios.

to the expansion of the cement paste due to the hydration temperature, whereas the decrease in the resistances is attributed to the shrinkage of the concrete due to loss of moisture. Fig. 11 shows that the maximum positive changes in the resistance occurred when the hydration temperature reached its maximum and the rate of change in these resistances depend mainly on the orientation of the resistors within the concrete. Resistors parallel to the longitudinal axes of the beam (angle=0°) exhibited the highest decrease in their resistance due to shrinkage and resistors parallel to the transversal axis of the beams exhibited the lowest decrease. Resistor orientation had a slight effect on the positive change during expansion.

The change in each resistor was used to calculate the principal shrinkage stresses using the piezoresistive theory developed for the sensor [4]. Fig. 12 shows a brief drop in the tensile stresses σ_1 and σ_2 (stresses due to cement expansion) that occurred when the specimens were removed from the molds. After the temperature and vapor pressure reached equilibrium, the measured tensile stresses increased slightly before gradually decreasing indicating that the shrinkage began thereby generating internal

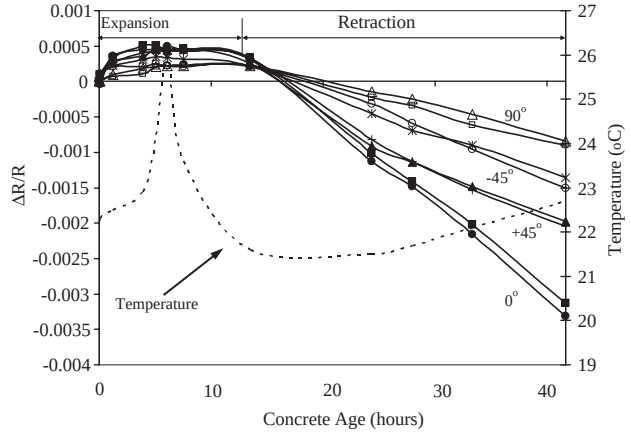

Fig. 11. Typical MEMS stress sensor response during concrete curing.

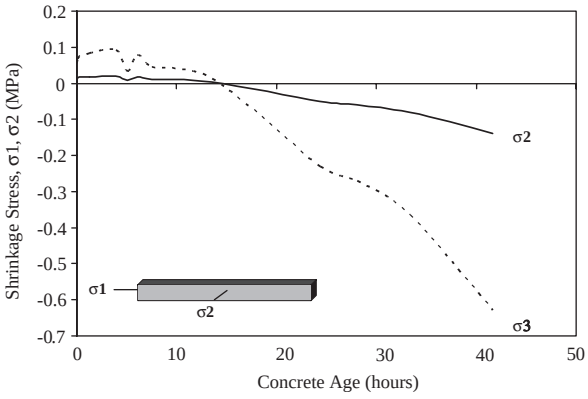

Fig. 12. Measured shrinkage stresses.

compressive stresses and these compressive stresses increased as the concrete dried. The compressive stress in the longitudinal axis increased more rapidly than that in the transversal axis.

The MEMS outputs showed clearly that the packaged die survived the corrosive concrete environment and there was no indication that the environmental condition affected the performance of the sensor in the concrete. The MEMS outputs reflect well the behavior of concrete during curing. Once calibrated, the MEMS moisture/temperature sensor outputs can be used to determine the relative humidity and temperature in concrete structures with high sensitivity.

To evaluate the effect of the external applied load on the sensors' outputs, at the end of the curing tests, the cylinders and beams were subjected to compression and three bending load respectively up to failure. The objective of these tests was to see whether the packaged sensors can survive the applied stress and to detect any anomaly in the dies during loading. Figs. 13 and 14 depict the MEMS moisture/temperature and stress sensors response during compression and three-bending tests respectively. The response of the

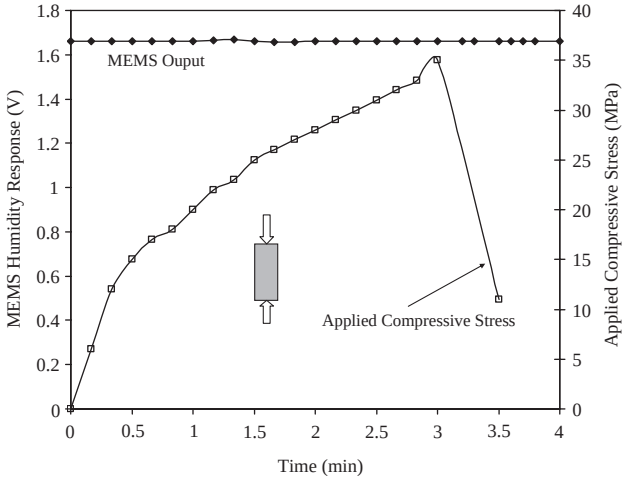

Fig. 13. Effect of applied compressive load on the MEMS moisture/temperature response.

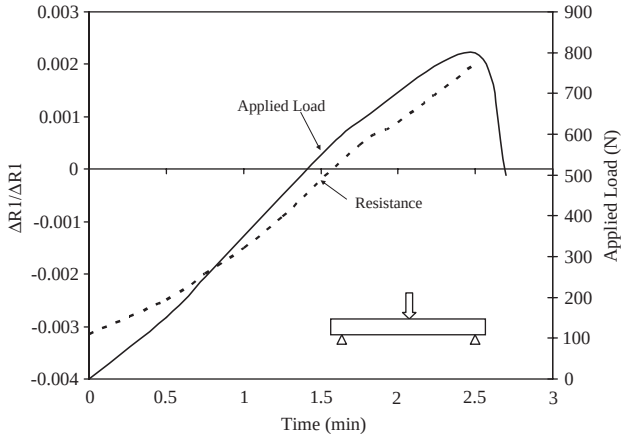

Fig. 14. Effect of three-point bending test on the MEMS stress sensor response.

MEMS stress sensor during loading is shown in terms of the change in the resistance of the microsensor $\frac{\Delta R_1}{R_1}$ placed parallel to the longitudinal axis of the beams. Tests showed that there was no change in the MEMS moisture/temperature sensor outputs and the sensor was recovered intact and used for other experiments. However, the MEMS stress sensor exhibited linear increase in the resistance R_1 due to the applied load. This is expected since the MEMS stress sensor was designed to measure shrinkage and load induced stresses.

Experimental tests are currently underway to further evaluate the durability of the performance of the proposed sensors and to develop the proposed wireless monitoring system for field application. In addition, these tests will be used to fully calibrate the proposed sensors as well as to develop analytical equations to predict in-place early age concrete strength gain based on the sensors' outputs.

5. Conclusions

In this paper, a cost effective wireless monitoring technique to monitor the behavior of concrete at early age is presented. Preliminary results indicated that the proposed MEMS sensors have a great potential application in concrete structures to continuously monitor their behavior with a minimum of cost and labor. Based on the obtained experimental results it was found that the proposed MEMS survived the concrete corrosive environment and internal and external stresses. Also it was found that the MEMS outputs reflect the change in the concrete properties and can be used to measure moisture content, temperature and shrinkage-induced stresses with a high sensitivity. Research is currently in progress to further evaluate the long-term durability of the sensors and determine their sensitivity and calibration equations. Analytical models to predict the strength gain using the sensors' outputs as well as the wireless monitoring technique are also currently being developed for field application.

Acknowledgement

The authors would like to acknowledge the financial support of the National Science Foundation Grant CMS 0216997. The authors also would like to thank Mr. Fenner, from Hygrometrix, Inc., for his technical support and recommendations.

References

[1] J.K. Kim, C.S. Lee, Moisture diffusion of concrete considering self-desiccation at early ages, Cem. Concr. Res. 29 (12) (1999) 1921–1927.

[2] B. Persson, Self-desiccation and its importance in concrete technology, Mater. Struct. 30 (199) (1997) 293–305.

[3] V. Slowik, E. Schlattner, T. Klink, Experimental investigation into early age shrinkage of cement paste by using fibre Bragg gratings, Cem. Concr. Compos. 26 (5) (2004) 473–479.

[4] M. Saafi, P. Romine, Embedded MEMS for health monitoring and management of civil infrastructure, Smart Materials and Structure, SPIE Proceedings, vol. 5391, SPIE, San Diego, California, 2004 (March 14–18), pp. 331–334.